

IMPACT OF A LARGE SAN ANDREAS FAULT EARTHQUAKE ON TALL BUILDINGS IN SOUTHERN CALIFORNIA

Swaminathan Krishnan ¹, Chen Ji ², Dimitri Komatitsch ³, and Jeroen Tromp ⁴

ABSTRACT

In 1857 a large earthquake of magnitude 7.9 (Sieh 1978b) occurred on the San Andreas fault with rupture initiating at Parkfield in Central California and propagating in a southeasterly direction over a distance of more than 360 km. Such a unilateral rupture produces significant directivity toward the San Fernando and Los Angeles basins. Indeed, newspaper reports (Agnew and Sieh 1978; Meltzner and Wald 1998) of sloshing observed in the Los Angeles river point to long-duration (1–2 min) and long-period (2–8 s) shaking, which could have a severe impact on present-day tall buildings, especially in the mid-height range. Using state-of-the-art computational tools in seismology and structural engineering, validated using data from the Northridge earthquake, we determine the damage in 18-story steel moment-frame buildings in southern California due to ground motion from a hypothetical magnitude 7.9 earthquake on the San Andreas fault. Our study indicates that serious damage occurs in these buildings at many locations in the region, leading to wide-spread building closures and seriously affecting the regional economy.

Introduction

The risk of earthquakes in southern California arises from two sources – well mapped-out faults such as the San Andreas, Newport-Inglewood, and Santa Monica-Hollywood-Raymond faults that have some form of surface expression, and the network of blind-thrust faults hidden deep inside the Earth that includes the Northridge fault and the Puente Hills fault under downtown Los Angeles. While the San Andreas strike-slip fault system has the potential for large (moment magnitude ~ 8) earthquakes, roughly every 200-300 years (Sieh 1978a; Sieh 1977), the blind-thrust faults have the potential for more moderate earthquakes (moment magnitude ~ 7). Fortunately, the urban areas of southern California have thus far been spared from the strongest shaking generated by large strike-slip earthquakes. However, the magnitude 6.7 earthquake of January 17, 1994, on the Northridge blind-thrust fault caused 57 deaths and economic losses in excess of \$ 40 billion (Eguchi et al. 1998; Petak and Elahi 2000). This earthquake exposed the vulnerability of steel moment-resisting frame buildings to fracture (SAC 1995a; SAC 1995b; SAC 1995c). These buildings resist lateral forces from an earthquake through bending in rigidly connected (welded) beams and columns. Due to certain

¹Seismological Laboratory, MC 252-21, California Institute of Technology, Pasadena, CA 91125, USA.

Email: krishnan@caltech.edu

²Seismological Laboratory, MC 252-21, California Institute of Technology, Pasadena, CA 91125, USA.

Now: Department of Geological Sciences, University of California, Santa Barbara, CA 93106, USA

³Department of Geophysical Modeling and Imaging, University of Pau, 64013 Pau Cedex, France

⁴Seismological Laboratory, MC 252-21, California Institute of Technology, Pasadena, CA 91125, USA

construction practices and the use of non-ductile weld material, a significant number of connections fractured in some of these buildings. Many of the moment-frame buildings in southern California were constructed before 1976 (EQE 1995), when there was inadequate understanding of the nature and power of earthquake forces and their effects on buildings. So the question arises as to what would happen to the many tall steel buildings in the mid-height range in the Los Angeles and San Fernando basins if a large earthquake were to occur on the San Andreas fault. Can we estimate damage and consequent losses in these buildings? There have been many improvements in building codes and construction practices since 1994, and buildings designed according to the latest code (1997 Uniform Building Code, UBC97, ICBO 1997), termed “new buildings” in this paper, are expected to perform far better than existing buildings, defined as those designed using codes preceding the UBC97, in large earthquakes. Will they in fact, and if so, is this performance adequate? Before we can answer these questions, we need to be able to answer more fundamental questions, e.g.: What kind of shaking would be experienced in this region during such an earthquake? What would the frequency content of the shaking be? What about the amplitude and duration of significant shaking?

In this study we combine state-of-the-art computational tools in seismology and structural engineering to perform an end-to-end 3D simulation of the rupture of a 290 km section of the San Andreas fault, the generation and propagation of the resulting seismic waves, the subsequent ground shaking in the Los Angeles and San Fernando basins, and the resulting damage to tall buildings in the region. A decade ago, Heaton et al. (Heaton et al. 1995; Hall et al. 1995; Hall 1998) simulated the near-source ground motions of a magnitude 7.0 thrust earthquake on a spatial grid of 60 km by 60 km using a vertically stratified crustal model that approximates the rock properties in the Los Angeles basin and then modeled the response of a 20-story steel-frame building and a 3-story base-isolated building. Olsen et al. (1995) and Graves (1998) simulated seismic wave propagation generated by a magnitude 7.75 earthquake on a different section of the San Andreas fault. Here we integrate many aspects of the earthquake-structure problem into a comprehensive end-to-end simulation by including the finite-source model of a real earthquake (Ji et al. 2002; Ji et al. 2003), 3D Earth structure (Komatitsch et al. 2004; Liu et al. 2004), 3D seismic wave propagation (Komatitsch and Tromp 1999), and 3D nonlinear damage analyses of buildings using three-component ground motion (Krishnan 2003b; Carlson 1999), validating these procedures using real data from recent earthquakes.

Figure 1 shows the domain of our analysis, which primarily includes the San Fernando and Los Angeles basins. The solid circles denote some of the major cities in the region. We have divided the region using a grid spaced at $1/32$ of a degree (about 3.5 km) each way. There is a total of 636 sites. We validate our procedure by performing a similar simulation for the Northridge earthquake and comparing our predictions against the limited available data.

Validation of Analysis Procedures

The magnitude 6.7 1994 Northridge earthquake was recorded at many stations in southern California and elsewhere. While many research groups have determined kinematic fault models by fitting seismic waveform data (Hartzell et al. 1996; Wald et al. 1996), we use a wavelet transform approach (Ji et al. 2002) that can extract more information about slip heterogeneity by simultaneously considering both the time and frequency characteristics of the waveforms. We

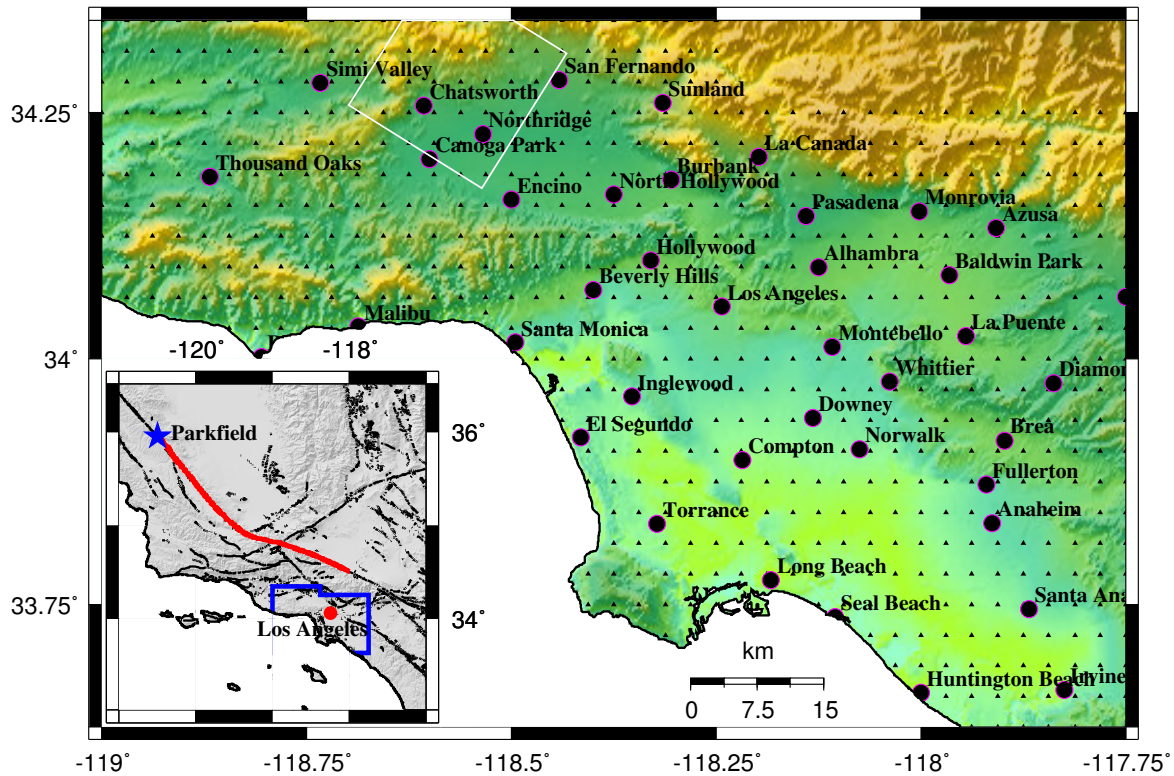


Figure 1: Geographical Scope of the Simulation (The color scheme reflects topography, with green denoting low elevation and yellow denoting mountains): The solid black triangles represent the 636 sites at which seismograms are computed and buildings are analyzed. The white box is the surface projection of the Northridge fault. The red line in the inset is the trace of the hypothetical 290 km rupture of the San Andreas fault that is the primary focus of this study. The area enclosed by the blue polygon denotes the region covered by the 636 sites.

use the spectral-element method (Komatitsch and Tromp 1999) that takes a deterministic approach to simulate ground motion⁵ generated by the resulting finite-source model of the Northridge earthquake.

For the Northridge simulation, in addition to the 636 sites under consideration, we compute seismograms at seismic stations in southern California that recorded the shaking during the earthquake. The synthetics (red) are compared against the recorded data (black) at distant stations (Figure 2A) and at nearby stations north of the fault (Figure 2B). All the waveforms are low-pass filtered at 2 s. The synthetics capture the large pulses in the nearby stations, and there is a wiggle-for-wiggle match in most waveforms corresponding to distant stations.

⁵In the deterministic approach, the elastic wave equation is solved in a realistic 3D Earth model and the ground motion is directly computed without any additional assumptions. In the case of the Los Angeles basin, the accuracy and frequency limitations depend on the accuracy of the 3D Los Angeles basin model, which has improved progressively in the last decade. For our study, we have used one of the two well-accepted 3D Southern California structures (the Harvard-LA model, the other being the SCEC Community Velocity Model, both of which allow us to model the basin response down to 2 s). The numerical simulations, accounting for 3D variations of seismic wave speeds and density, topography and bathymetry, and attenuation, are carried out using our open-source seismic wave propagation package SPECFEM3D (<http://www.geoframework.org>). The methodology adopted therein has been shown to reliably model ground motion down to a period of approximately 2 s (Komatitsch et al. 2004; Liu et al. 2004).

While there is a sufficient amount of ground motion data to validate the seismological component of our procedure, the same is not true of tall building performance. Not many tall buildings in the region were instrumented at the time. One building that was instrumented was an 18-story steel moment-frame building in Woodland Hills built in 1984. Many connections in the lateral force-resisting moment-frames of this building fractured (SAC 1995b). There was a 3-component accelerometer on the 18th floor of the building that recorded the floor acceleration (Darragh et al. 1994). Unfortunately, the closest free-field seismometer was at the Oxnard Boulevard station (WHOX) located in Woodland Hills, located about half-a-mile away from the building. The building model was analyzed for shaking from the recorded three-component ground motion. This nonlinear damage analysis of the structure was performed using a 3D finite-element program, FRAME3D⁶.

The computed displacements at the 18th floor in the North-South and East-West directions are compared against the corresponding measured displacements in Figures 2C and 2D. The computed peak displacement in the North-South direction is within 5% of the measured displacement. However, the peak displacement in the East-West direction is off by a factor of 2. There is a minor lengthening of the period in the measured displacement that is not captured by the computed displacements. Also, the measured displacement attenuates faster than the computed displacement. These differences could be due to any or all of the following reasons: the ground motion used in the analysis was not recorded at the base of the building but half-a-mile away; the instrument at the roof was maintained by the owner and its reliability is uncertain; rocking of the building about its base (due to the finite stiffness of the soil), which is not included in the fixed-base structural model, could contaminate the displacement record measured at the roof and the observed period may actually be a combination of purely translational and rocking modes; as damage accumulates in a building during an earthquake, (non-hysteretic) damping increases significantly. However, in our structural model, while hysteretic damping is modeled accurately in a non-linear fashion, non-hysteretic supplemental damping is considered to be viscous and linear, and as damage accumulates, it does not increase correspondingly.

For this building, and for others in its class whose dominant modes of vibration have natural periods greater than 2 s, high-frequency ground motion does not have a significant impact on the structural response. To confirm this, we have analyzed the two buildings considered in the study for three-component unfiltered and low-pass filtered records observed from the 1999 Chi-Chi (Taiwan) and 2001 Tokachi-Oki (Japan) earthquakes. The primary structural response parameter that is used to evaluate structural performance is the interstory drift, which is the difference in displacement between the top and bottom of a story normalized by its height. The interstory drift is a good indicator of the ability of a structure to resist $P - \Delta$ instability and collapse. It is also closely related to the plastic rotation demand

⁶The nonlinear time-history analyses of the building models are carried out using a finite element program, FRAME3D (Krishnan 2003a; Krishnan 2003b, <http://www.frame3d.caltech.edu>). The particular 3D elements used by the program to model beams, columns and joints in buildings have been shown to simulate damage therein accurately and efficiently. Material nonlinearity resulting in flexural yielding, strain-hardening and ultimately rupturing of steel at the ends of beams and columns, and shear yielding in the joints (also known as panel-zones) is included (Krishnan and Hall 2006a; Krishnan and Hall 2006b). The FRAME3D program incorporates geometric nonlinearity, which enables the modeling of the global stability of the building, accounting for $P - \Delta$ effects accurately. The fracture mode of failure is included in connections, however, local flange buckling in beams and columns is not. Column splices can be incorporated into the model, but are excluded in this study. Soil-structure interaction is not included in the analyses.

on individual beam-column connection assemblies, i.e., the greater the yielding in the beams, columns and joints, the greater this interstory drift would be, reducing the stability of the building. For each of the records considered, we plot the peak interstory drift computed in the building due to the filtered records against that computed in the corresponding unfiltered record (Figure 2E). If the high-frequency ground motion had no effect whatsoever on the response of the buildings, all the points would fall on the diagonal. The fact that most of the points are aligned quite closely with the diagonal indicates that the effect of higher-frequency ground motion on the response of the tall buildings considered here is not significant and band-limited simulated ground motions can indeed be reliably used for the analysis of the tall buildings considered in this study.

San Andreas Earthquake Simulation

For the San Andreas simulation, it is critical to have a realistic source model (slip distribution in time along and across the fault). The Denali fault system in Alaska is geometrically similar to the San Andreas fault. On November 3, 2002, a magnitude 7.9 earthquake occurred on this fault system. It initiated as a magnitude 7.1 thrust event on the Susitna Glacier fault, quickly changed to a strike-slip mode of rupture and propagated southeastward along the Denali fault for 218 km before jumping to the Totschunda fault and continuing further for about 76 km (Eberhart-Phillips et al. 2003). We have studied the slip distribution of this earthquake using teleseismic body waves and strong motion waveforms as well as GPS vectors (Ji et al. 2003). Here, we have mapped the slip on the Denali and Totschunda faults (290 km long), amounting to a moment magnitude of 7.9, on to the San Andreas fault, the rupture starting at Parkfield and progressing in a southeasterly direction a distance of about 290 km (Figure 1 inset). The maximum depth of rupture is about 20 km. The surface slip grows slowly to 7.4 m and drops off drastically towards the end of the rupture, which incidentally is contrary to what happened in the 1857 San Andreas earthquake, where the slip along the fault is deduced to have grown quickly to a peak value of about 9.5 m and then dropped off gradually (Sieh 1978b). The peak slip at depth is about 12 m, and the peak particle velocity is $4.3 \text{ m}\cdot\text{s}^{-1}$.

Using the spectral-element method, we compute seismograms at each of the 636 hypothetical tall-building sites (Figure 1). The minimum S wave velocity in the basin model is $687 \text{ m}\cdot\text{s}^{-1}$. The horizontal size of the mesh cells at the surface is approximately 270 m in each direction. The resulting number of grid points per S wavelength is about 5. The time step used for the computations is 0.009 s, with a total number of 30000 steps, i.e., a total duration of 270 s. Shown in Figures 3A and 3B are maps of the peak velocity and displacement of the strong (E-W) component of ground motion low-pass-filtered at 2 s. The solid circles in these maps correspond to the cities shown in Figure 1. The San Fernando valley experiences severe shaking. As the rupture proceeds down south from Parkfield and hits the bend in the San Andreas fault, it sheds off a significant amount of energy into the region that is directly in front of it, which happens to be the San Fernando valley (see <http://www.ce.caltech.edu/krishnan> for a movie of the rupture and seismic wave propagation). A good portion of this energy spills over into the Los Angeles basin, with many cities along the coast such as Santa Monica and Seal Beach and more inland areas going East from Seal beach towards Anaheim experiencing long-duration shaking. In addition, the tail-end of the rupture sheds energy from SH/Love

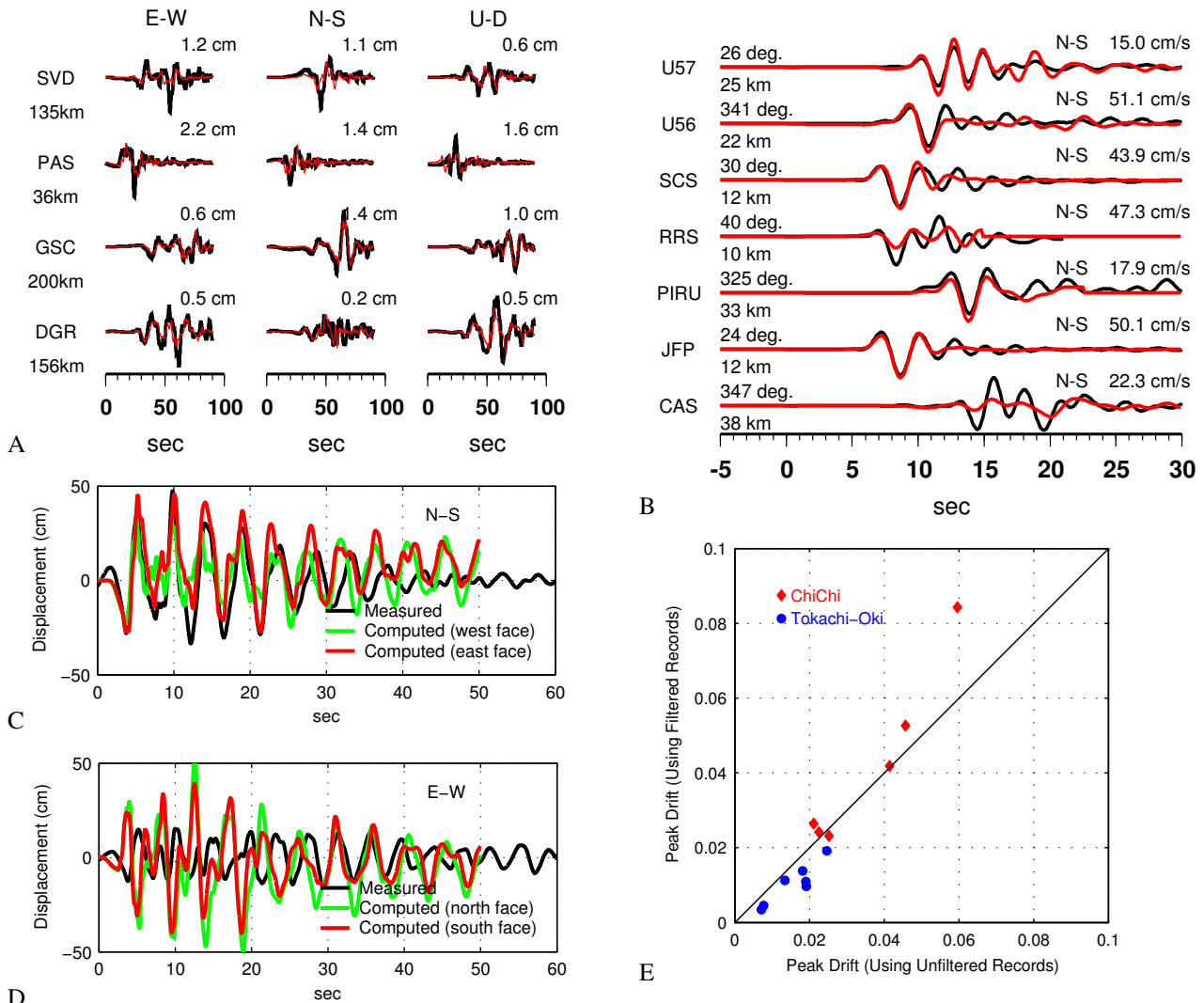


Figure 2: Northridge Simulation (A-D): [A] Data (black) versus synthetics (red) – Distant stations. [B] Data versus synthetics – Nearby stations north of the rupture. The waveforms shown form a representative sample of the data inventory. [C] and [D] Measured 18th floor North-South and East-West displacements versus corresponding computed displacements using the unfiltered WHOX record – Existing building in Woodland Hills. [E] Analyses of the existing building to unfiltered and low-pass filtered records from the 1999 Chi-Chi (Taiwan) and the 2001 Tokachi-Oki (Japan) earthquakes: Computed peak drifts in the building using filtered records versus that using unfiltered records. The close alignment of all the points with the diagonal for all damage ranges indicates that the effect of higher-frequency ground motion (periods < 2 s) on the response of the tall buildings considered in this study is not significant and can be safely ignored.

waves into the Baldwin Park-La Puente region, which is bounded by a line of mountains that creates a mini-basin, further amplifying the ground motion. The peak velocity is of the order of 1 m.s^{-1} in the Los Angeles basin, including downtown Los Angeles, and 2 m.s^{-1} in the San Fernando valley. The map of peak displacements has characteristics quite similar to that of the peak velocities, with significant displacements in the basins but not in the mountains. The peak displacements are in the neighborhood of 1 m in the Los Angeles basin and 2 m in the San Fernando valley.

Building Performance and Discussion

To study the effects of the simulated ground motion on tall buildings located at each of the 636 sites shown in Figure 1, we analyze computer models of the existing building in Woodland Hills described earlier as well as a building with the same configuration but redesigned according to the latest building code (ICBO 1997). The 1997 code regulations specify larger design forces and call for greater redundancy in the lateral force-resisting system. This results in a greater number of bays of moment-frames (Krishnan et al. 2005). As before, the analyses are performed using the FRAME3D program (Krishnan 2003a). We use the peak interstory drift to evaluate structural performance. The Federal Emergency Management Agency (FEMA) proposes limits ⁷ on the peak drift ratio for classifying building performance.

In the existing building, we also take into account the fracture mode of failure in the beam-to-column connections that was widely observed during the Northridge earthquake. The fracture index represents the percentage of connections in the building that fractured. Since the Northridge earthquake, this defect has been corrected and we do not expect this mode of failure to happen in buildings built today.

To put our results on existing buildings in perspective, note that while the population of tall buildings in southern California is quite widespread, a major fraction is located in downtown Los Angeles, the mid-Wilshire district (Beverly Hills), west Los Angeles, and Santa Monica. There are quite a few tall buildings spread across the San Fernando valley as well, e.g., in Woodland Hills and Canoga Park, and 30-40 tall buildings in Orange County (comprising the cities of Orange, Irvine, Costa Mesa, Newport Beach, Anaheim, Santa Ana, Garden Grove, etc.). A host of new tall buildings are being planned in Orange County with the cities of Anaheim and Sanata Ana leading the way with thirteen proposed high-rises.

⁷Since there is very little usable data to assess the performance of tall buildings based on calculated drifts, we take an empirical approach proposed by the Federal Emergency Management Agency (FEMA). For rehabilitation of existing buildings, FEMA 356 (FEMA 2000a) defines three performance levels. Immediate Occupancy (IO) refers to a post-earthquake damage state in which very limited structural damage has occurred. The risk of life-threatening injury as a result of structural damage is very low, and although some minor structural repairs may be appropriate, these would generally not be required prior to reoccupancy. Life Safety (LS) is a post-earthquake damage state that includes damage to structural components but retains a margin against onset of partial or total collapse. Collapse Prevention (CP) refers to a post-earthquake damage state that includes damage to structural components such that the structure continues to support gravity loads but retains no margin against collapse. The interstory drift limits for the IO, LS, and CP performance levels as specified by FEMA are 0.007, 0.025, and 0.05, respectively. For the design of new steel moment-frame buildings, FEMA 350 (FEMA 2000b) defines only two performance levels, the IO and CP levels. For buildings taller than 12 stories, the interstory drift limits for these levels as specified therein are 0.01 and 0.06, respectively.

The results of our building analyses (see <http://www.ce.caltech.edu/krishnan> for movies of buildings swaying under the earthquake resulting in permanent tilt or collapse) corresponding to a north-to-south rupture of the San Andreas fault are summarized in Figures 3C through 3F for the existing 18-story steel building and Figures 3G through 3I for the new 18-story steel building. Figure 3C shows the percentage of connections where fracture occurs in the existing building. Fracture occurs in at least 25% of the connections in this building when located in the San Fernando valley. Note that the scale saturates at 25% and that this number is exceeded at many locations. About 10% of the connections fracture in the building when it is located in downtown Los Angeles and the mid-Wilshire district (Beverly Hills), while the numbers are about 20% when it is located in Santa Monica, west Los Angeles, Inglewood, Alhambra, Baldwin Park, La Puente, Downey, Norwalk, Brea, Fullerton, Anaheim and Seal beach. Figures 3G through 3I show the peak interstory drift that occurs in the top-third, middle-third, and bottom-third of the existing building, respectively. The fact that the peak interstory drifts in the middle-third and bottom-third of the existing building are far greater than the top-third indicates that the damage is localized in the lower floors. The localization of damage in the lower floors rather than the upper floors could potentially be worse because of the risk of more floors pancaking on top of each other if a single story gives way. Consistent with the extent of fracture observed, the peak drifts in the existing building exceed 0.10 when it is located in the San Fernando valley, Baldwin Park and neighboring cities, Santa Monica, west Los Angeles and neighboring cities, Norwalk and neighboring cities, and Seal Beach and neighboring cities, which is well into the postulated collapse regime. Note that the scale saturates at 0.10, and in fact the drifts far exceed this number in many locations in these regions. When located in downtown Los Angeles and the mid-Wilshire district, the building would barely satisfy the collapse prevention criteria set by FEMA (FEMA 2000a; FEMA 2000b) with peak drifts of about 0.05.

The performance of the newly designed 18-story steel building is significantly better than the existing building for the entire region. However, note that the new building has significant drifts indicative of serious damage when located in the San Fernando valley or the Baldwin Park area. When located in coastal cities (such as Santa Monica, Seal Beach etc.), the Wilshire corridor (west Los Angeles, Beverly Hills, etc.), the central Los Angeles basin region (Downey, Norwalk, etc.) or the booming Orange County cities of Anaheim and Santa Ana, it has peak drifts of about 0.05, once again barely satisfying the FEMA collapse prevention criteria (FEMA 2000a; FEMA 2000b). In downtown Los Angeles it does not undergo much damage in this scenario. Thus, even though this building has been designed according to the latest code, it suffers damage that would necessitate closure for some time following the earthquake in most areas, but this should be expected since this is a large earthquake and building codes are written to limit the loss of life and ensure “collapse prevention” for such large earthquakes, but not necessarily limit damage. Unfortunately, widespread closures such as this could cripple the regional economy in the event of such an earthquake.

It should be mentioned that for the north-to-south rupture of the San Andreas fault considered here, had the slip distribution along the fault been like the 1857 earthquake, i.e., rising quickly to the peak value and then gradually dropping off (Sieh 1978b), instead of the other way around, results could have been quite different, with greater amount of energy possibly being directed into the San Fernando valley. Also, directivity can have a significant impact on ground shaking and the resulting building damage. For example, for a south-to-north rupture of the same earthquake,

building damage is far less severe (Krishnan et al. 2005).

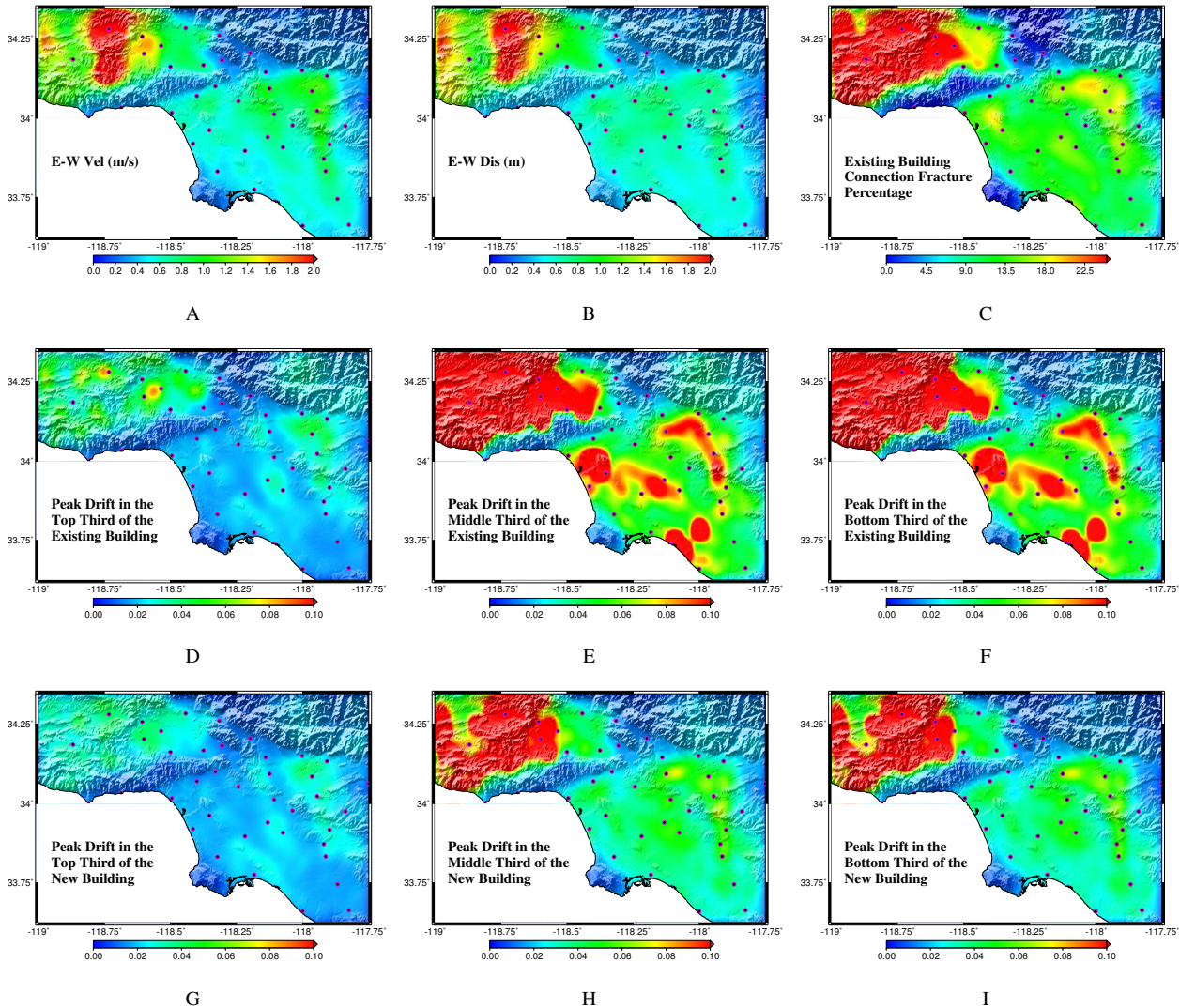


Figure 3: M_w 7.9 Earthquake (North-to-South Rupture) on the San Andreas Fault – Ground shaking and building performance: Shown in this figure are the peak ground velocity [A] and displacement [B] of the synthetics low-pass filtered with a corner period of 2 s, the percentage of connections in the existing building where fractures occur [C], the peak interstory drift in the top [D], middle [E] and bottom-third [F] of the existing building, and the corresponding peak drifts for the new building ([G], [H], and [I], respectively). Peak interstory drifts beyond 0.06 are indicative of severe damage, while drifts below 0.01 are indicative of minimal damage not requiring any repairs.

Finally, the building analyses herein are specific to steel moment-frame buildings in the mid-height range. Other buildings with varied configuration, constructed with other materials, and having varied dynamic characteristics could have damage patterns quite different from the results presented here. Having said this, the fact remains that the potential for a large earthquake with a large amount of slip on the San Andreas fault exists, and with our current state of knowledge of the southern Californian Earth structure, our study indicates that serious damage occurs in tall steel moment-frame buildings in the mid-height range in at least one of the plausible scenarios.

References

- Agnew, D. C. and K. Sieh (1978). A documentary study of the felt effects of the great California earthquake of 1857. *Bulletin of the Seismological Society of America* 68(6), 1717–1729.
- Carlson, A. (1999). Three-dimensional nonlinear inelastic analysis of steel moment-frame buildings damaged by earthquake excitations. Technical Report EERL 1999-02, Earthquake Engineering Research Laboratory, California Institute of Technology, California.
- Darragh, R., T. Cao, V. Graizer, A. Shakal, and M. Huang (1994). Los Angeles code-instrumented building records from the Northridge, California earthquake of January 17 1994: Processed release No. 1. Technical Report OSMS 94-17, California Strong Motion Instrumentation Program, California Department of Conservation, Division of Mines and Geology (now California Geological Survey).
- Eberhart-Phillips, D., P. J. Haeussler, J. T. Freymueller, A. D. Frankel, C. M. Rubin, P. Craw, N. A. Ratchkovski, G. Anderson, G. A. Carver, A. J. Crone, T. E. Dawson, H. Fletcher, R. Hansen, E. L. Harp, R. A. Harris, D. P. Hill, S. Hreinsdottir, R. W. Jibson, L. M. Jones, R. Kayen, D. K. Keefer, C. F. Larsen, S. C. Moran, S. F. Personius, G. Plafker, B. Sherrod, K. Sieh, N. Sitar, and W. K. Wallace (2003). The 2002 Denali fault earthquake, Alaska: A large magnitude, slip-partitioned event. *Science* 300, 1113–1118.
- Eguchi, R. T., J. D. Goltz, C. E. Taylor, S. E. Chang, P. J. Flores, L. A. Johnson, H. A. Seligson, and N. C. Blais (1998). Direct economic losses in the Northridge earthquake: A three-year post-event perspective. *Earthquake Spectra* 14(2), 245–264.
- EQE (1995). The Northridge earthquake of January 17, 1994: Report of data collection and analysis, Part A: Damage and inventory data. Technical Report EQE Project No. 36386.02, EQE International Inc. and the Geographic Information Systems Group of the Governor's Office of Emergency Services.
- FEMA (2000a). *Prestandard and Commentary for the Seismic Rehabilitation of Buildings*. FEMA-356. Federal Emergency Management Agency, USA.
- FEMA (2000b). *Recommended Seismic Design Criteria for New Steel Moment-Frame Buildings*. FEMA-350. Federal Emergency Management Agency, USA.
- Graves, R. W. (1998). Three-dimensional finite-difference modeling of the San Andreas fault: Source parameterization and ground-motion levels. *Bulletin of the Seismological Society of America* 88(4), 881–897.
- Hall, J. F. (1998). Seismic response of steel frame buildings to near-source ground motions. *Earthquake Engineering and Structural Dynamics* 27, 1445–1464.
- Hall, J. F., T. H. Heaton, M. Halling, and D. Wald (1995). Near-source ground motion and its effects on flexible buildings. *Earthquake Spectra* 11(4), 569–605.
- Hartzell, S. H., P. Liu, and C. Mendoza (1996). The 1994 Northridge, California, earthquake: Investigation of rupture velocity, rise time, and high-frequency radiation. *Journal of Geophysical Research* 101(B9), 20091–20108.

- Heaton, T., J. Hall, D. Wald, and M. Halling (1995). Response of high-rise and base-isolated buildings to a hypothetical M_w 7.0 blind thrust earthquake. *Science* 267, 206–211.
- ICBO (1997). *1997 Uniform Building Code*. Volume 2. International Conference of Building Officials, Whittier, California.
- Ji, C., Y. Tan, D. Helmberger, and J. Tromp (2003). Modeling teleseismic P and SH static offsets for great strike-slip earthquakes. In *Proceedings of the American Geophysical Union Fall Meeting*.
- Ji, C., D. J. Wald, and D. V. Helmberger (2002). Source description of the 1999 Hector Mine, California, earthquake – Part I: Wavelet domain inversion theory and resolution analysis. *Bulletin of the Seismological Society of America* 92(4), 1192–1207.
- Komatitsch, D., Q. Liu, J. Tromp, P. Suss, C. Stidham, and J. H. Shaw (2004). Simulations of ground motion in the Los Angeles basin based upon the spectral-element method. *Bulletin of the Seismological Society of America* 94, 187–206.
- Komatitsch, D. and J. Tromp (1999). Introduction to the spectral-element method for three-dimensional seismic wave propagation. *Geophys. J. Int.* 139, 806–822.
- Krishnan, S. (2003a). FRAME3D – A program for three-dimensional nonlinear time-history analysis of steel buildings: User guide. Technical Report EERL 2003-03, Earthquake Engineering Research Laboratory, California Institute of Technology.
- Krishnan, S. (2003b). Three-dimensional nonlinear analysis of tall irregular steel buildings subject to strong ground motion. Technical Report EERL 2003-01, Earthquake Engineering Research Laboratory, California Institute of Technology, California.
- Krishnan, S. and J. F. Hall (2006a). Modeling steel frame buildings in three dimensions – Part I: Panel zone and plastic hinge beam elements. *Journal of Engineering Mechanics, ASCE (Scheduled for publication in April 2006)*.
- Krishnan, S. and J. F. Hall (2006b). Modeling steel frame buildings in three dimensions – Part II: Elastofiber beam element and examples. *Journal of Engineering Mechanics, ASCE (Scheduled for publication in April 2006)*.
- Krishnan, S., C. Ji, D. Komatitsch, and J. Tromp (2005). Performance of 18-story steel moment-frame buildings during a large San Andreas earthquake – a Southern California-wide end-to-end simulation. Technical Report EERL 2005-01, Earthquake Engineering Research Laboratory, California Institute of Technology, Pasadena, California, USA.
- Liu, Q., J. Polet, D. Komatitsch, and J. Tromp (2004). Spectral-element moment tensor inversions for earthquakes in Southern California. *Bulletin of the Seismological Society of America* 94(5), 1748–1761.
- Meltzner, A. J. and D. J. Wald (1998). Foreshocks and aftershocks of the great 1857 California earthquake. Technical Report USGS Open-File Report 98-465, United States Department of the Interior, USGS, Pasadena, California.

- Olsen, K. B., R. J. Archuleta, and J. R. Matarese (1995). Three-dimensional simulation of a magnitude 7.75 earthquake on the San Andreas fault. *Science* 270, 1628–1632.
- Petak, W. J. and S. Elahi (2000). The Northridge earthquake, USA, and its economic and social impact. In *Euro-Conference on Global Change and Catastrophe Risk Management, Earthquake Risks in Europe*, IIASA, Laxenburg, Austria.
- SAC (1995a). Analytical and field investigations of buildings affected by the Northridge earthquake of January 17, 1994 – Part 1. Technical Report SAC 95-04, Part 1, Structural Engineers Association of California, Applied Technology Council, and California Universities for Research in Earthquake Engineering.
- SAC (1995b). Analytical and field investigations of buildings affected by the Northridge earthquake of January 17, 1994 – Part 2. Technical Report SAC 95-04, Part 2, Structural Engineers Association of California, Applied Technology Council, and California Universities for Research in Earthquake Engineering.
- SAC (1995c). Surveys and assessments of damage to buildings affected by the Northridge earthquake of January 17, 1994. Technical Report SAC 95-06, Structural Engineers Association of California, Applied Technology Council, and California Universities for Research in Earthquake Engineering.
- Sieh, K. E. (1977). *A Study of Late Holocene Displacement History Along the South-Central Reach of the San Andreas Fault*. Ph. D. thesis, Stanford University, California.
- Sieh, K. E. (1978a). Pre-historic large earthquakes produced by slip on the San Andreas fault at Pallett creek, California. *Journal of Geophysical Research* 83, 3907–3939.
- Sieh, K. E. (1978b). Slip along the San Andreas fault associated with the great 1857 earthquake. *Bulletin of the Seismological Society of America* 68(5), 1421–1448.
- Wald, D. J., T. H. Heaton, and K. W. Hudnut (1996). A dislocation model of the 1994 Northridge, California, earthquake determined from strong-motion, GPS, and leveling-line data. *Bulletin of the Seismological Society of America* 86, S49–S70.